Experimental evaluation of a hybrid adsorption-compression cascade chiller for solar cooling applications in industrial processes

Valeria Palomba[1*], Giuseppe E. Dino[1], Steffen Kühnert[2], Davide La Rosa[1], Andrea Frazzica[1]

[1] CNR ITAE, Salita S. Lucia sopra Contesse 5, 98126, Messina, Italy

[2] Fahrenheit GmbH, Siegfriedstr. 19, 80803 Munich, Germany

Abstract

The present work reports the experimental evaluation of the performance of a cascade chiller, having an adsorption cycle as topping cycle and a vapour compression cycle as bottoming cycle. An experimental testing campaign was carried out at CNR ITAE, focused on the definition of performance maps of the system under different operating conditions. In particular, heat source temperatures between 70°C and 85°C were evaluated, cooling temperatures between 22°C and 40°C and chilled water temperatures of -12°C up to 5°C, in order to reproduce the operation in different seasons, climates and user requests (i.e. air conditioning and refrigeration). Cooling powers from 18 kW (under air conditioning conditions) from 12 kW (for refrigeration conditions) were obtained for the lower cooling temperatures. Indeed, the cooling temperature has a great influence on the cooling capacity of the system, whereas heat source temperature has a smaller effect on the capacity of the system. Finally, the energy savings that can arise from such a configuration were calculated and up to 25% reduction, if compared to a standard vapour compression system can be achieved. A reduction in CO_2 emissions up to 3.5 yearly tons were calculated as well.

Keywords: industrial refrigeration; adsorption; natural refrigerants; experimental

1. Introduction

Cooling demand of industrial processes accounts for a significant amount of energy in different sectors (Werner, 2016). For this reason, the integration of renewable thermal energy sources inside industrial sites, for both heating and cooling applications is gaining a lot of attention (Farjana et al., 2018; Montagnino, 2017). Usually, it is accomplished with the use of thermally driven chillers, i.e. adsorption or absorption chillers (Murray et al., 2016). However, thermal chillers suffer from some disadvantages, such as the discontinuous behaviour, which produces a non-constant cold supply to the user, and the poor performance at high ambient temperature. Moreover, their capital cost is higher than traditional vapour compression chillers, limiting the application when a high power needs to be installed. On the contrary, hybrid cascade chillers exploiting the coupling between vapour compression and adsorption chiller can benefit from the good regulation capabilities of the electric unit and the low primary energy consumption of the thermal unit, increasing up to 40% the efficiency of the system (Salvatore Vasta et al., 2018). In such a background, the EU co-funded project HyCool (HyCool, 2018) aims at increasing the use of solar heat in industrial processes, integrating a concentrating Fresnel solar thermal collector technology, with a hybrid cascade chiller, to increase the share of renewable sources for heating and cooling applications in industries. A first design of the cascade chiller to be realised was presented in (Palomba et al., 2018), together with a preliminary control strategy. In the present work, the experimental characterization at CNR ITAE lab is presented.

2. The investigated chiller

The hybrid chiller tested consists of two units connected in cascade: an adsorption module employing silica gel/water as working pair and a compression chiller using R1270 as refrigerant. Therefore, one of the peculiarities of the hybrid machine is the use of natural and low Global Warming Potential (GWP) refrigerants: the adsorption unit makes use of R718 (water), with 0 GWP and 0 Ozone Depletion Potential (ODP); the compression unit makes use of R1270 (propylene) with GWP=2 and 0 ODP. The two units work in cascade, meaning that the chilled water circuit from the adsorption chiller represents the cooling water circuit of the compression chiller. The connection between them is made through a hydraulic circuit. The schematics of the concept proposed is presented in Figure 1, together with a rendering of the hybrid chiller. The acronyms used for the circuits of the hybrid system are shown in Figure 1 as well.

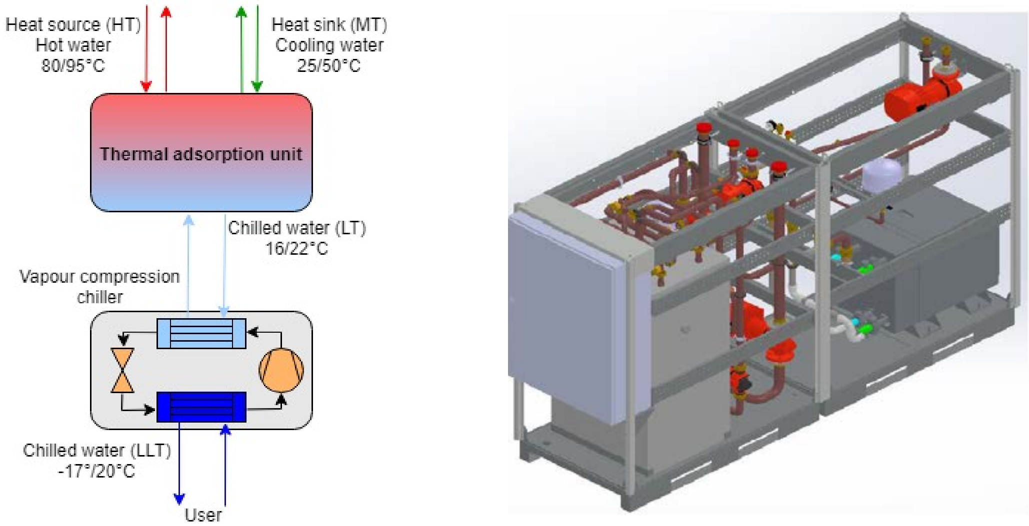

Figure 1: schematic layout of the hybrid heat pump and rendering of the system.

3. Experimental facilities

The testing rig used for the evaluation of the performance of the hybrid chiller is specifically designed to set the different thermal levels required for the operation of thermal and hybrid components. It mainly consists of heat sources and sinks connected to storages: a 1.5 m^3 water storage, continuously heated up by a 70 kW heater (HT storage); a 1 m^3 water storage connected to an air-cooled chiller with nominal power of 63 kW (LT storage) and a 0.75 m^3 storage filled with a 40%wt. water/glycol mixture (LLT storage) where 5 immersed resistances (3kW each) are placed for temperature control. It has to be pointed out that, in the framework of HYCOOL project, the testing rig was upgraded to comply with the request of providing refrigeration at temperature below 0°C. This was obtained by installing the new LLT storage, equipped with the electrical resistances to control the temperatures.

The HT (heat source) circuit of the Fahrenheit unit is connected directly to the HT storage; the MT (cooling water circuit of the adsorption chiller) sink is obtained by mixing the water in the HT and LT storages with a motorised 3-way valve connected to a PID regulator. The LLT circuit of the compression chiller (chilled water circuit) is directly connected to the LLT storage. All the circuits are thermally insulated and are equipped with variable speed pumps that can be used for the testing of prototypes that do not include them. The operation and management of the testing rig are accomplished thanks to a control panel realised in LabVIEW® environment. The testing rig is equipped with the sensors listed in Table 3.

- Type "T" thermocouples with Class 1 tolerances for the measure of all the temperatures in the inlet/outlet pipes of every circuits and in the storages;
- Magnetic flow meters with 1% of reading accuracy for the measure of all the flow rates;
- Piezoresistive differential pressure meter, to calculate pressure drops inside the circuits of the heat pumps/chillers under testing;
- Electric energy meter with Class 1 tolerances for the measure of electric input delivered to the chillers.

A picture of the testing rig, with the main components indicated is shown in Figure 2, whereas Figure 3 shows the system installed in the lab of CNR ITAE.

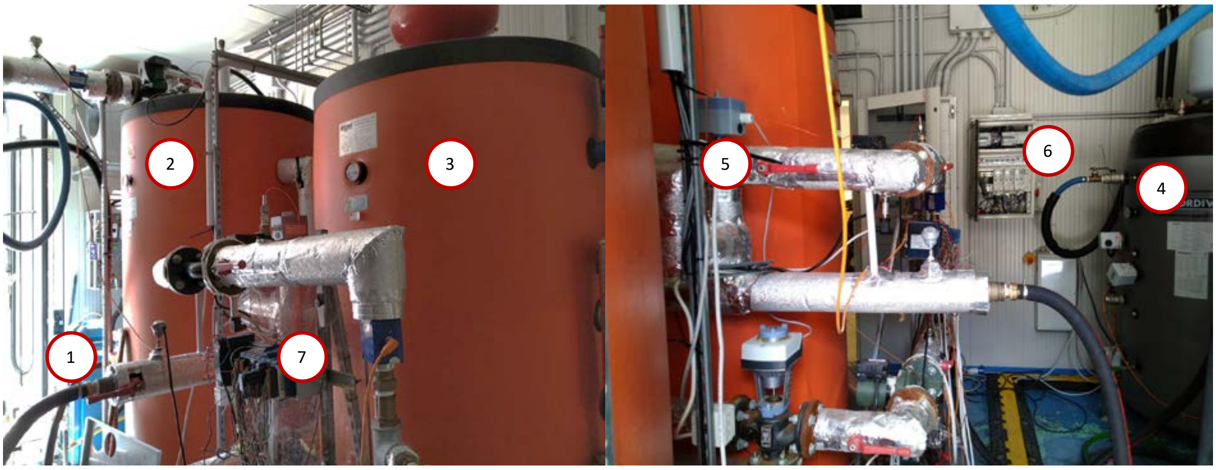

Figure 2: the testing rig at CNR-ITAE. 1: heat source; 2: HT storage; 3: LT storage; 4: LLT storage; 5: mixing valve MT circuit; 6: electric cabinet; 7: data acquisition system.


Figure 3: the chiller connected to the testing rig at CNR ITAE.

4. Data reduction

System performance was estimated after the calculation of the following parameters:

- Heating power provided to the adsorption chiller Q_{HT};
- Heat rejection power of the adsorption chiller Q_{MT};
- Cooling energy provided by the electric chiller Q_{LText};
- Electrical energy input for the operation of the compression chiller and the auxiliaries of the hybrid system P_{el}.

The instantaneous power for each component were calculated as:

$$\dot{Q} = \dot{m} c_p (T_{in} - T_{out}) \quad (1)$$

Where $\dot{Q}$ is the instant power in kW, $\dot{m}$ is the mass flow rate in the circuit in kg/s, c_p is the specific power of the heat transfer fluid and T_{in} and T_{out} are the inlet and outlet temperatures of the circuit considered.

The EER of the whole hybrid system is defined as the ratio between the overall cooling energy provided by the compression unit during the test, and the overall electric consumption. This term takes into account the electric consumption of the compression chiller, the controller of the adsorption chiller and all the pumps included in the cascade unit.

$$EER_{cascade} = \frac{\int_0^{\tau_{test}} \dot{m}_{LText} c_p (T_{LText\_in} - T_{LText\_out}) d\tau}{\int_0^{\tau_{test}} \mathrm{P}_{el} d\tau} \quad (2)$$

The EER gain is defined as. the ratio between the EER of the cascade chiller and the EER of the reference system, i.e. the EER of the compression unit working as a stand-alone unit and directly cooled down by the dry cooler The EER calculated in both cases takes into account the electric consumption of the pumps needed for the operation of the system. Indeed, the electric consumption of the auxiliaries only was measured as well. It amounts to 2.3 kW, of which about 0.3 kW are due to the consumption of the controllers of the two units and the remaining part can be ascribed to the pumps of the system. It is also worth noticing that, for the tests presented, a water/glycol 40%wt mixture was used in the LLT circuit, in order to avoid freezing even when very low temperatures are set, but in real applications mixtures with lower glycol amount can be used, which in turn reduces the viscosity of the heat transfer fluid and the electric consumption of the auxiliaries.

$$EER_{gain,overall} = \frac{EER_{cascade}}{EER_{reference}} \quad (3)$$

5. Results

The chiller was fully characterized by examining the effect of operating conditions on the cooling capacity and the EER of the cascade chiller. Different heat source temperatures, cooling temperatures and chilled water outlet temperatures were investigated, with the aim of building a map of performance of the system. The nominal flow rates suggested by the producers of the sorption and compression units were set in all the circuits. Some of the results obtained are presented in Figure 4, where the cooling power and EER are reported as a function of MT temperature (cooling temperature), for different HT (heat source temperatures) and different chilled outlet temperatures of the compression unit of the cascade (LLT). The EER considered in all the graphs and comments is the $EER_{cascade}$ calculated according to Eq. 2 and the HT and MT temperatures indicate refer to the inlet values. There is a clear linear trend in both the cooling power and EER with the MTin: increasing the ambient temperature leads to a loss in efficiency and cooling capacity of the system. In particular, for a chilled outlet of -5°C, the cooling power that the cascade can deliver ranges from 15 kW (at 21°C MTin) to 10 kW (at 40°C MTin), with an EER (including the consumption of the auxiliaries) between 4 and 2. For evaporation temperatures above 0°C (i.e .LLT between 2°C and 5°C, as reported in Figure 4b), the cooling power that the cascade can deliver is between 18.7 kW (at 20°C and with an heat source temperature of 80°C) and 15.5 kW (at 37°C and an heat source temperature of 80°C). The corresponding EERs are 4 and 2.5. Lowering down the heat source temperature from 80°C to 70°C, the cooling power ranges between 17.6 kW and 14.5 kW, with corresponding EERs of 3.7 at MTin=21°C to 2.4 at MTin=37°C. It is worth highlighting that the heat source temperature does not significantly influence the performance: regardless of the parameter and temperature levels, passing from 85°C to 70°C introduces a penalisation in the performance of the chiller around 10%, both for EER and cooling capacity. Such a reduction of cooling capacity and EER with the temperature is slightly higher for higher evaporation temperatures (around 15% f for LLT of 0°C and above), whereas at lower temperatures, it reduces down to around 8%. Such a result is strictly dependent from the choice of the sorbent in the adsorption unit, i.e. silica gel that can be effectively regenerated also at lower temperatures. This is an important outcome since it proves the reliability of the chiller also under conditions in which solar resource is not optimal (first and last hours of the day, partially cloudy days, northern latitudes) and indicates a high flexibility of the solution proposed.

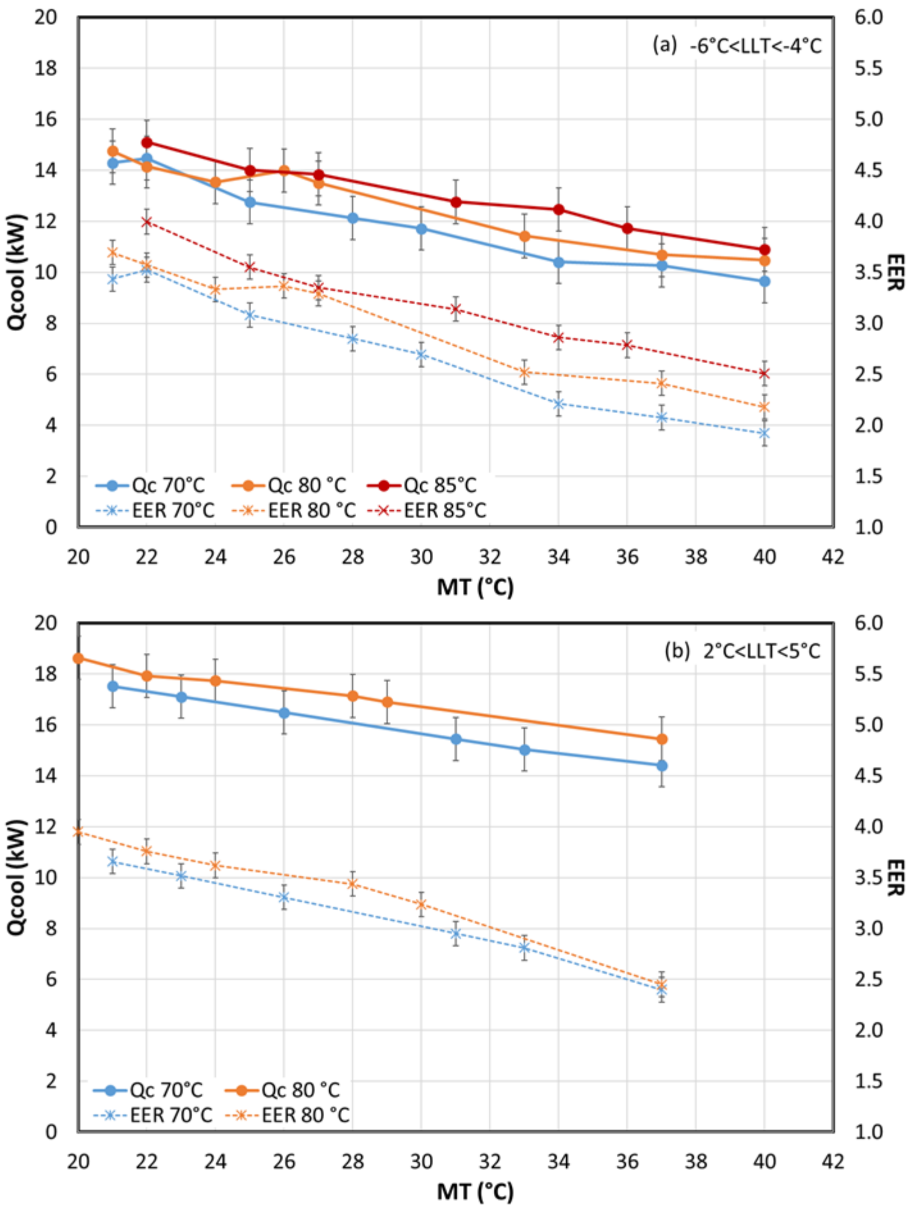

Figure 4: effect of operating conditions on the cooling power and EER: (a) LLT between -6°C and -4°C; (b) LLT between +2°C and +5°C.

The results of the tests were further converted into performance maps, useful for the easy visualization and identification of the expected performance of the system, in terms of cooling power and EER. The performance maps regarding the cooling power and EER for an HTin interval of 77-82°C are shown in Figure 5. As it is possible to notice, the range of LLT tested is from -14°C to 5°C, whereas cooling temperatures of 21°C to 40°C were investigated. The maps are characterized by vertical bands, thus demonstrating the combined effect of evaporation and condensation temperatures. In agreement with the measurements shown before, increasing the MT temperature, induces a linear reduction of the cooling power and EER of the system. The LLT has a similar effect, even though less marked than the MT temperature. For the lower evaporation temperatures, the effect of MT temperature is slightly less noticeable than for the case of higher evaporation temperatures, due to the approximation to the limits for the operation of the compression unit.

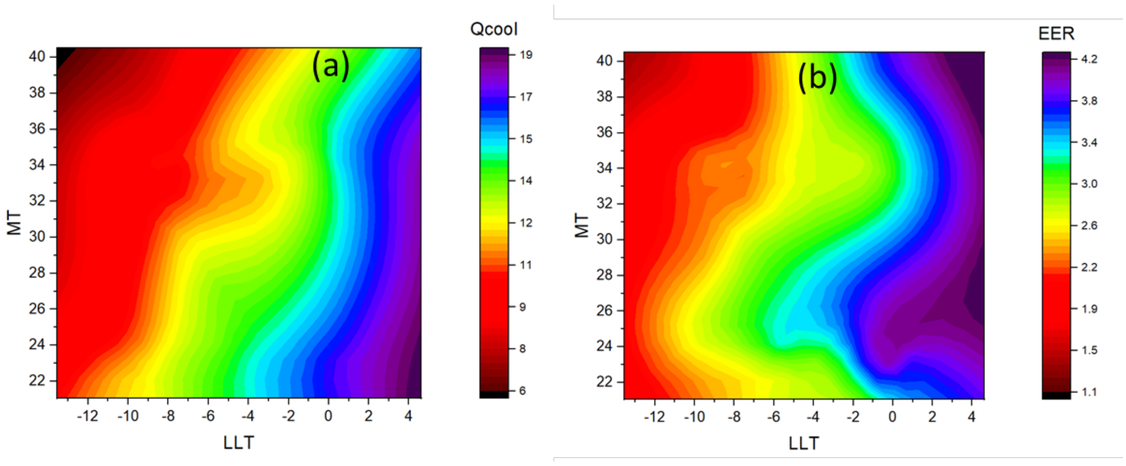

Figure 5: performance maps of the hybrid chiller. (a) Cooling power; (b) EER.

6. Environmental analysis

In order to calculate the energy savings, the operation of the system was compared to a reference system, i.e. the compression chiller working as a stand-alone unit and directly cooled down by the dry cooler. To evaluate the electric consumption of the compression chiller in such a condition, the performance table from the GEA VAP tool, supplied by the producer of the compressor, was used. The effect of operating the compression unit in cascade mode is twofold: on the one side, for a given MT temperature, the cooling power that the hybrid system can produce is higher than the reference system; on the other side, the electric consumption is lower. To highlight such an effect, the amplification factor σ was calculated. It is defined as the ratio between the cooling power of the cascade and the cooling power provided by the compression unit in the reference system, i.e. as a stand-alone unit:

$$\sigma = \frac{Q_{LText_{cascade}}}{Q_{LT_{reference}}} \qquad (4)$$

Figure 6a shows the amplification factor for the same temperature intervals considered in the characterization of the system. It is possible to notice that the increment in the cooling power delivered goes from 15% to 30% and increases with the increasing condensation temperature. The EERgain, as defined by Eq. (3), is shown in Figure 6b. The trend is similar to that of the amplification factor: for increasing cooling temperature, the advantage in the use of the hybrid chiller over the stand-alone compression leads to an increase in the EER up to the 70%. In particular, considering typical winter conditions, i.e. 22°C MT temperature, it is possible to notice that the increase in EER is between 50% and 65%, whereas, in typical summer conditions, i.e. cooling temperatures of 35°C, this is about 70%. The EER measured for the hybrid when HT=80°C, MT=22°C, LLT=-5°C is 5.4, which is a clear advancement over the use of traditional systems. Under summer operation conditions, at HT=80°C, MT=32°C, LLT=-5°C, the measured EER (without the consumption of the auxiliaries) is 4.5, also in this case, with a gain of up to 50% compared to traditional heat pumps in the same power size (S. Vasta et al., 2018). If we add also the consumption of auxiliaries, the EER in winter conditions is 4.4 and the EER in summer conditions is 3.2, still guaranteeing a higher efficiency than in the case of the reference system.

In addition, the electricity savings were calculated as:

$$E_{saved}[\%] = \left(\frac{P_{el_{reference}} - P_{el_{cascade}}}{P_{el_{reference}}}\right)\sigma \qquad (5)$$

Where the correction with the amplification factor was used, to take into account that, under the same conditions, a higher cooling capacity is provided.

The results are shown in Figure 6C: savings up to 25% can be achieved in summer conditions and up to 22%

in winter conditions. More interestingly, the savings achieved are similar for air conditioning and refrigeration conditions, thus showing the flexibility of the system.

Finally, CO_2 emissions avoided were calculated under the assumptions of 6000 h of yearly working period and in comparison to R134a, which is the refrigerant typically used in standard systems. The amount of GHG emissions avoided is:

$$\Delta CO_2 = \Delta E_{el} \cdot EF_{CO2} + m_{R134a} * GWP_{R134a} \cdot leakage\_rate \qquad (8)$$

Where the refrigerant charge of 60 g/kW for R134a, with a leakage rate of 10% was considered (Corberan, 2014). The GWP value of R134a was considered equal to 1300 (Protocol, 2016) and the emission factor for EU-28 is 0.393 (Covenant, n.d.).

The results are shown in Figure 6d: up to 3.5 t of emissions can be avoided yearly, thus strengthening the benefits of the HYCOOL hybrid system.

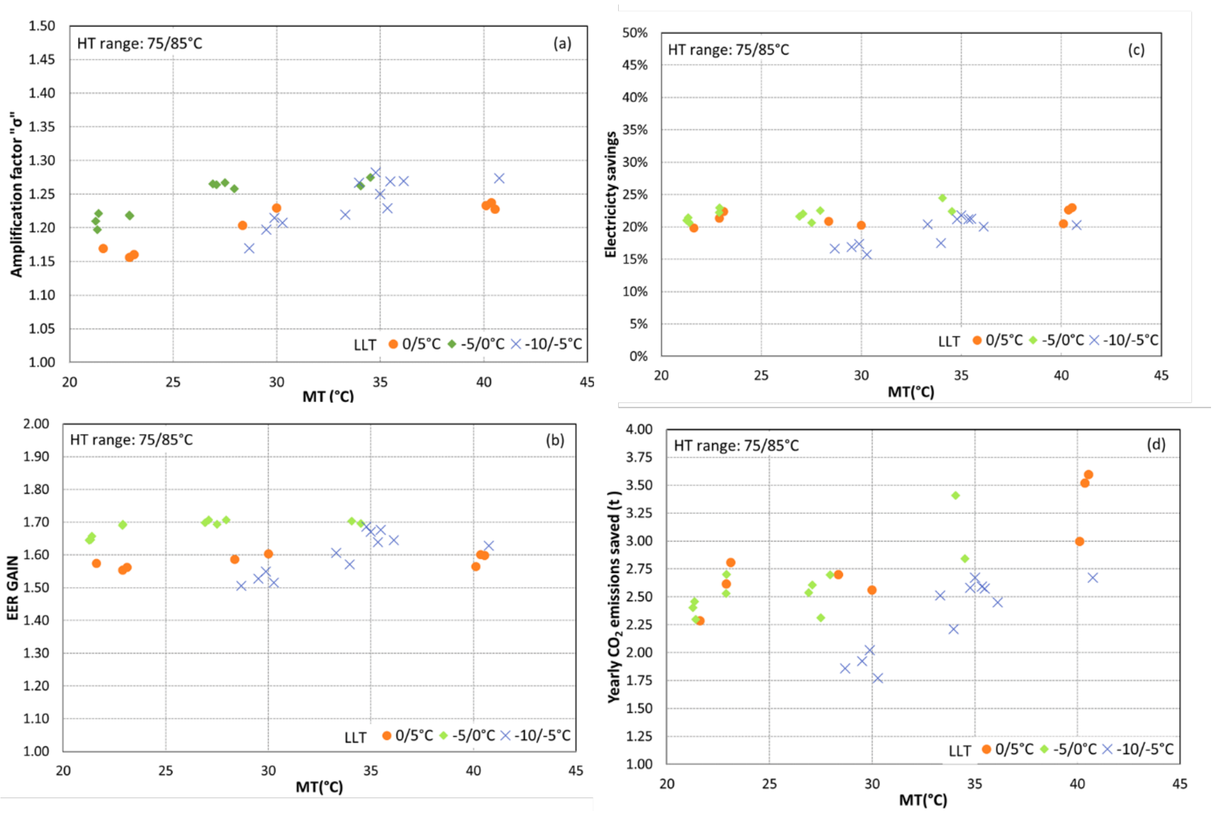

Figure 6:results of the environmental analysis (a) amplification factor for different boundary conditions; (b) EER gain; (c) energy savings;(d) CO_2 emissions saved.

7. Conclusions

A cascading hybrid chiller was tested under controlled boundary conditions reproducing the operation in different seasons, climates and user requests (i.e. air conditioning and refrigeration). The main outcomes of the analysis are summarized below:

- The overall performances are only slightly affected by the driving temperature level, indeed, in general, passing from 85°C to 70°C, a performance reduction in terms of EER is around 10% on average.
- The parameters which affect more the chiller efficiency are the condensation temperature (i.e. the ambient temperature) and the evaporation temperature (i.e. the cooling temperature to deliver to the load).
- The chiller is able to provide cooling power with an appreciable EER, around 2.5 when the ambient temperature is 30°C, even at -11°C. This confirms the ability of the machine to operate far from the nominal conditions.

- The calculated electricity energy savings range from 15% to 25%, depending on the operating conditions. Similarly, the expected CO_2 yearly emissions saved range from 2.0 up to 3.5 ton/ for a machine with nominal cooling capacity of 22 kW.

8. Acknowledgements

This project has received funding from the European Union's Horizon 2020 research and innovation programme under grant agreement No 792073 (HYCOOL).

9. References

Corberan, J.M., 2014. 25th Informatory Note on Refrigeration Technologies.

Covenant, E.M., n.d. National and European Emission factors [WWW Document]. URL https://www.eumayors.eu/IMG/pdf/technical_annex_en.pdf

Farjana, S.H., Huda, N., Mahmud, M.A.P., Saidur, R., 2018. Solar process heat in industrial systems – A global review. Renew. Sustain. Energy Rev. 82, 2270–2286. https://doi.org/10.1016/J.RSER.2017.08.065

HyCool, 2018. HyCool [WWW Document].

Montagnino, F.M., 2017. Solar cooling technologies. Design, application and performance of existing projects. Sol. Energy. https://doi.org/10.1016/j.solener.2017.01.033

Murray, C., Quiñones, G., Cortés, F., Escobar, R., Cardemil, J.M., 2016. Solar Assisted Absorption Machine for the Fermentation Cooling and Maceration Heating Processes in the Winemaking Industry. Energy Procedia 91, 805–814. https://doi.org/10.1016/J.EGYPRO.2016.06.247

Palomba, V., Frazzica, A., Kühnert, S., Große, A., 2018. Experimentally validated dynamic model for a hybrid cascade system for solar heating and cooling applications, in: EuroSun2018. Rapperswill 20-23 september 2018.

Protocol, G., 2016. Global Warming Potential Values [WWW Document]. URL https://www.ghgprotocol.org/sites/default/files/ghgp/Global-Warming-Potential-Values %28Feb 16 2016%29_1.pdf

Vasta, Salvatore, Palomba, V., La Rosa, D., Mittelbach, W., 2018. Adsorption-compression cascade cycles: An experimental study. Energy Convers. Manag. 156, 365–375. https://doi.org/10.1016/j.enconman.2017.11.061

Vasta, S., Palomba, V., La Rosa, D., Mittelbach, W., 2018. Adsorption-compression cascade cycles: An experimental study. Energy Convers. Manag. 156, 365–375. https://doi.org/10.1016/j.enconman.2017.11.061

Werner, S., 2016. European space cooling demands. Energy 110, 148–156. https://doi.org/10.1016/J.ENERGY.2015.11.028